

Understanding the Spectral Bias of Coordinate Based MLPs Via Training Dynamics

John Lazzari^{a,*} and Xiuwen Liu^b

^aFlorida State University, Department of Mathematics

^bFlorida State University, Department of Computer Science
ORCID ID:

Abstract.

Spectral bias is an important observation of neural network training, stating that the network will learn a low frequency representation of the target function before converging to higher frequency components. This property is interesting due to its link to good generalization in over-parameterized networks. However, in applications to scene rendering, where multi-layer perceptrons (MLPs) with ReLU activations utilize dense, low dimensional coordinate based inputs, a severe spectral bias occurs that obstructs convergence to high frequency components entirely. In order to overcome this limitation, one can encode the inputs using high frequency sinusoids. Previous works attempted to explain both spectral bias and its severity in the coordinate based regime using Neural Tangent Kernel (NTK) and Fourier analysis. However, such methods come with various limitations, since NTK does not capture real network dynamics, and Fourier analysis only offers a global perspective on the frequency components of the network. In this paper, we provide a novel approach towards understanding spectral bias by directly studying ReLU MLP training dynamics, in order to gain further insight on the properties that induce this behavior in the real network. Specifically, we focus on the connection between the computations of ReLU networks (activation regions), and the convergence of gradient descent. We study these dynamics in relation to the spatial information of the signal to provide a clearer understanding as to how they influence spectral bias, which has yet to be demonstrated. Additionally, we use this formulation to further study the severity of spectral bias in the coordinate based setting, and why positional encoding overcomes this.

1 Introduction

In the last several years, neural networks have increasingly been employed to provide a way to learn representations that generalize well in dense, low dimensional domains. Specifically in the field of computer graphics, coordinate based multi-layer perceptrons (MLPs) with ReLU activations have been vital for applications such as neural radiance fields (NeRF) [13] and shape occupancy [12]. These networks pass in dense, low dimensional input coordinates, and output the corresponding scene representation of color, shape, or density for various visual signals. Note that a coordinate based MLP is a standard ReLU MLP, and its name is simply derived from the task it is given. Coordinate based MLPs are intriguing due to their severe spectral bias, meaning they are practically incapable of learning the high frequency



Figure 1: Visualization of the large spectral bias induced by dense low dimensional 2D coordinates (a), which is overcome by a high frequency positional encoding (b-c). For this task, the coordinate based MLP is tasked with regressing the RGB value corresponding to the 2D pixel location, or its sinusoidal embedding. Coordinate based inputs have difficulty converging to the high frequency components of the image, and can only generate a smooth, low frequency representation.

components of the target signal [13]. This limitation can be overcome through a positional encoding of coordinates $\mathbf{v} \in \mathbb{R}^d$ comprised of high frequency sinusoids:

$$\gamma(\mathbf{v}) = \left[\sin(2^0 \pi \mathbf{v}), \cos(2^0 \pi \mathbf{v}), \dots, \sin(2^L \pi \mathbf{v}), \cos(2^L \pi \mathbf{v}) \right],$$

where $L \in \mathbb{N}$ determines the maximum frequency [23, 20]. This behavior raises two important questions: What properties of neural network training dynamics (specifically ReLU) induce spectral bias, and why does it become so severe in dense, low dimensional settings?

Spectral bias is the behavior such that neural networks learn a simpler, lower frequency representation of the target function before converging to the high frequency components, or finer details. This phenomenon is of interest due to its impact on generalization, since it is believed that an implicit regularization biased towards lower frequency solutions avoids overfitting in over-parameterized networks [19]. While spectral bias is generally believed to aid in generalization, in the coordinate based regime it becomes so severe that the network will essentially underfit the target signal (see Figure 1 for more details).

Further understanding the nature of spectral bias will be crucial in determining its impact on generalization. So far, Neural Tangent Kernel (NTK) [9] and Fourier analysis have been the primary tools for analyzing spectral bias, both in the coordinate based regime and more generally [23, 19]. While NTK models gradient descent dynamics via a kernel method (whose kernel matrix becomes a constant in the

* Corresponding Author. Email: jcl19h@fsu.edu.

limit of very wide layers), the dynamic properties of the real network are not accurately captured. On the other hand, the Fourier decomposition of a ReLU network is bounded by the total number of linear regions as well as its Lipschitz constant [19], which does provide real network insights. Spectral decay rates of parameter gradients have been found as well. However, this only provides a global perspective on the network properties, mostly through upper bounds, thus the local dynamics of the network that induce spectral bias have yet to be demonstrated.

In this paper, we take a different approach towards understanding spectral bias. Our contributions are as follows:

- We develop a novel framework for understanding spectral bias through real network training dynamics, which incorporates ReLU network computations, gradient descent convergence, as well as the spatial information of the signal. Specifically, we relate the network’s expressive capacity (activation regions) with the ability to speed convergence of gradient descent, through a metric termed gradient confusion [22]. We find more confusion (slower convergence) when expressive power between inputs is limited, and less confusion (faster convergence) when expressive power is enhanced. This results in slower convergence to the local details of the signal, where inputs are typically restricted to the same or nearby activation regions.
- We use this formulation to explore the severity of spectral bias in the coordinate based regime, and how positional encoding overcomes this. We find that positional encoding greatly enhances expressive capacity across the signal, resulting in faster convergence to high frequency components. We provide additional analysis as well, by studying the unique properties of the activation regions as encoding frequency increases, and exposing the dying ReLUs that occur in the low dimensional setting.

Note that the scope of this paper lies within the regression setting similar to previous work, and not more complex settings such as classification, since spectral bias is still largely unexplored in these areas. We additionally focus on the case of uniformly distributed inputs (coordinate regime), which has been fairly standard as well.

The paper is structured as follows. Section 2 provides related work. In Section 3, we define activation regions and explore how density restricts the expressive capacity of the network. Section 4 discusses gradient confusion, and connects confusion to the network’s activation regions. In Section 5, we analyze the properties of the activation regions induced by higher frequency encodings, and Section 6 demonstrates how dense coordinates turn off ReLU neurons during training. Section 7 is a conclusion which details future directions for this approach.

2 Related Work

In [19, 3], it was shown that neural networks have a bias towards learning low frequency functions first, referred to as spectral bias, and that a sinusoidal mapping can allow for higher frequencies to be learned faster. This method was adopted by NeRF [13] in order to speed converge of high frequency components during novel view synthesis. As a consequence of this, the relationship between coordinates and positional encoding was analyzed by the same authors using NTK [23]. They found that the eigenspectrum of the NTK decays rapidly with dense coordinates, and widens for positional encoding. This allows for faster convergence along the directions of the corresponding eigenfunctions. Our work can best be seen as an extension

of [23], however we also focus on real network dynamics, and use this to confirm the results found using NTK with positional encoding.

Aside from its severity in coordinate based MLPs, spectral bias has been studied independently due to its link to good generalization in over-parameterized networks. [19] provide the first rigorous exploration of spectral bias using Fourier analysis. In [4], it was shown how the eigenfunctions of the NTK have their own convergence rate given by their corresponding eigenvalue, using inputs with uniform density on \mathbb{S}^1 . The authors in [3] also utilized NTK to give convergence rates for inputs of non-uniform density in \mathbb{S}^1 . There has been a line of work referring to spectral bias as the F-principle [24], in which Fourier analysis was utilized for high dimensional inputs in sigmoidal nets. Other works have attempted to compute spectral bias and determine convergence rates as well [10, 21]. Note that these works largely focus on gaining insights from MLPs in the regression regime.

Our analysis of spectral bias utilizes activation/linear regions. Exploring the complexity of functions computable by piece-wise linear networks initially explored in [17]. This approach was expanded upon in [14], where upper and lower bounds for the maximal number of linear regions was given, and shown to be exponential with depth. In [18], activation regions were defined, and bounds were computed by utilizing input trajectories $x(t)$ across the regions. More recently, [7, 8] attempted to compute practical bounds for the number of activation regions, which was found to be independent of depth. [26] provides useful experimental quantities for studying the properties of linear regions in a more practical manner.

In this paper, we relate expressive capacity to the correlation of gradients during training. We specifically focus on gradient confusion [22], which was found to be higher in deeper networks, making them more difficult to train if their width does not increase concurrently. Other works have utilized correlations between gradients in different settings as well [2, 6, 25].

3 Expressive Power

3.1 Experimental Setting

We begin our study by exploring activation regions, and providing experimental details. In Section 4 (main results), we conduct experiments on natural images using a four layer MLP with 512 hidden neurons, where results are averaged over five images from the div2k dataset [1]. Regressing these images has been a common benchmark in recent works on positional encoding [23, 5]. We also provide results averaged over five randomly generated 1D sinusoids

$$\gamma(x) = \sum_i A_i \sin(2\pi k_i x + \phi_i)$$

for $k = (5, 10, \dots, 70)$, with 2048 uniform input samples normalized in $[0, 1]$ similar to [19]. We use equal amplitudes $A_i = 1$ and randomly sampled phases $\phi_i \sim \mathcal{U}(0, 2\pi)$. This task uses a four layer network with 128 hidden neurons. For both tasks we use the Adam optimizer [11] with a learning rate of .001 and mini-batches. Unless otherwise stated, all other results in this paper are averaged over the same five images using the four layer, 512 hidden neuron architecture.

3.2 Activation Regions

We analyze the expressive power of a neural network with dense and uniform inputs through its activation regions. We begin by defining activation regions and patterns. Let $f_\theta : \mathbb{R}^{n_{\text{in}}} \rightarrow \mathbb{R}^{n_{\text{out}}}$ be a continuous piece-wise linear function given by a ReLU network containing

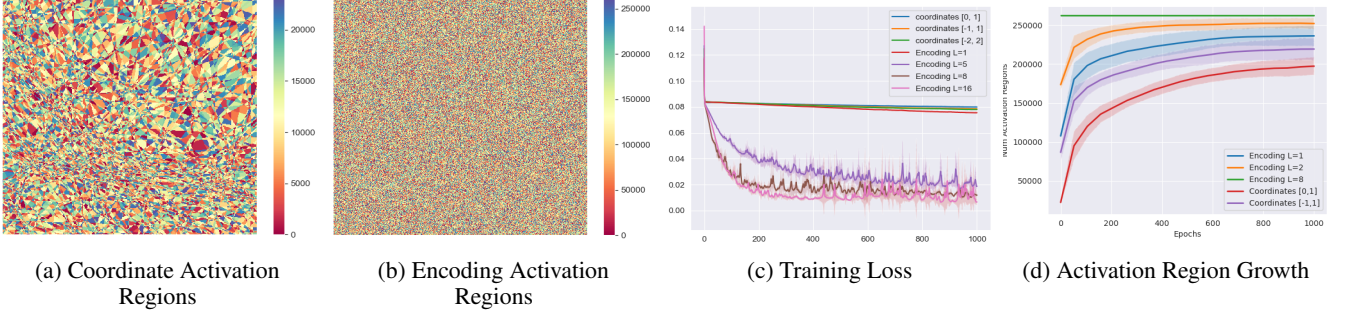


Figure 2: Visualization of the regions in which each input belongs to (a-b) (colored according to unique region) at the beginning of training. Many coordinates lie in the same activation regions, but positional encoding allows for each input to lie in a unique activation region. In (c), we show the training losses of different encoding frequencies as well as coordinates, and in (d) we plot the number of unique activation patterns created as training progresses. We only focus on the activation patterns utilized for the given dataset (512x512 total regions), and demonstrate how coordinate based inputs and low frequency encodings are unable to map each input to a unique activation region throughout training.

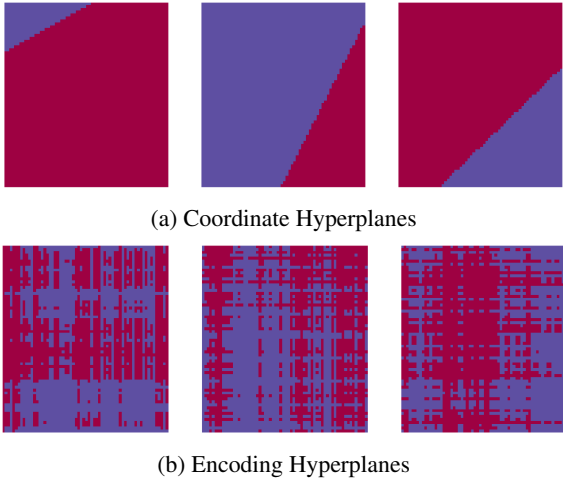


Figure 3: Visualization of the hyperplanes in the first layer for coordinates and positional encoding. The encoding hyperplanes are projected back to 2D.

L hidden layers with N hidden neurons per layer. The network is defined as the composition of affine transformations $f_l(x) = \mathbf{W}^l x + \mathbf{b}^l$ with ReLU activations $\sigma = \max(0, f_l)$ such that

$$f_\theta = f_{\text{out}} \circ \sigma \circ f_L \circ \sigma \circ \dots \circ \sigma \circ f_1(x),$$

where θ denotes the vector of trainable parameters. Each neuron $z_i^l(x) = \mathbf{W}_i^l x + \mathbf{b}_i^l$ composed with σ denotes a hyperplane equation with the scalar determined by the bias. The collection of these hyperplanes in the first layer gives a hyperplane arrangement in $\mathbb{R}^{n_{\text{in}}}$, splitting the input space into pieces that compute distinct linear functions. As the image of each distinct linear function in the preceding layer $l-1$ is uniquely partitioned by the following neurons $z_i^l(x)$ (or not), the $N-1$ dimensional hyperplanes in layers $l > 1$ will appear to bend. Overall, this leads to a ReLU network partitioning the input space into convex polytopes on which unique linear functions are computed. One way to evaluate these polytopes is through activation regions, which are determined by the network’s activation patterns, defined as

Definition 1 (Activation Pattern). Let f_θ be a ReLU network, and $z_i^l(x)$ denote the pre-activation of a neuron in the l th layer. Then, an activation pattern \mathcal{A} of the network is a vector in $\{0, 1\}^{\#\text{neurons}}$

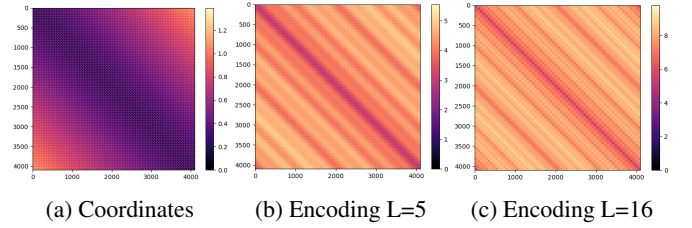


Figure 4: Matrix of coordinate distances (a) and encoding distances (b-c) for different frequencies. Positional encoding induces a kernel with a strong diagonal since it is stationary.

composed of neuron activations such that 0 is assigned if $z_i^l(x) < 0$ and 1 if $z_i^l(x) > 0$.

Definition 2 (Activation Region). For a ReLU network f_θ , the activation regions \mathcal{R} of f_θ are the sets of input samples that correspond to the same \mathcal{A} ,

$$\mathcal{R}(f, \mathcal{A}) = \{x \in \mathbb{R}^{n_{\text{in}}} \mid \mathbb{1}_{\mathbb{R}^+}(\text{ReLU}(f^l(x))) = a_l, \forall l \in 1, \dots, k, \forall a_l \in \mathcal{A}\}$$

where a_l is the activation pattern of layer l .

Analyzing activation regions are important because they provide a measure of the expressive power of the network, or the complexity of functions it can compute. In [8], a realistic upper bound on the maximum number of activation regions created by a ReLU network architecture was given as

$$\frac{\#\text{Regions in } \mathcal{F} \text{ intersecting } \mathcal{C}}{\text{vol}(\mathcal{C})} \leq \frac{(TN)^{n_{\text{in}}}}{n_{\text{in}}!} \quad (1)$$

where N is the number of neurons, T is a constant, and \mathcal{C} is a cube in input space.

Equation (1) is determined by the number of neurons and the input dimension. Therefore, the dimensionality of the inputs themselves show that the network with positional encoding should have more expressive capacity. However, input density is a major factor as well, therefore we also analyze how the network utilizes its activation regions across the dataset, since focusing solely on the total number of regions would not provide insight on the local dynamics of the network. We can define the set of interest on a dataset $\mathcal{D} = \{x_i, y_i\}_{i=1}^n$, given in terms of the corresponding activation patterns as

$$\mathcal{L}_{\mathcal{D}} = \{\mathbb{1}_{\mathbb{R}^+}(\text{ReLU}(f^l(x))) \mid x \in \mathcal{D}, \forall l \in 1, \dots, k\},$$

equipped with the hamming distance $\sum_{i=1}^n |a_i - b_i|$, for $a, b \in \mathcal{L}_{\mathcal{D}}$ to determine their distinctiveness. We later use hamming distance as a proxy for determining expressive power between inputs (higher distance, more expressive power).

3.3 Comparisons

In Figure 2, we get a glimpse of the limitations imposed by dense, low dimensional inputs. The number of activation regions utilized with coordinates is lower than the number of elements in the dataset (Fig. 2 (a,b)), meaning many inputs will be regressed using the same linear function. This restriction holds throughout training (Fig. 2(d)). On the other hand, positional encoding can easily map each element to a unique activation region using the same architecture. The hyperplane arrangements in the first layer are displayed in Figure 3, demonstrating the complex higher dimensional split that positional encoding allows in two dimensions as opposed to coordinates. Overall, we can see that coordinate based inputs have very little expressive power during training in comparison to positional encoding.

The reasoning for this reduced expressive power is a result of both density and a lack of activation regions in low input dimensions. Coordinates impose a grid over a subset of \mathbb{R}^d in which the resolution, given by their spacing, is very fine-grained. Therefore, fitting enough neurons in the first layer such that a substantial amount of hyperplanes can separate each input becomes difficult. If the input to layers $l > 1$ are restricted to the images of similar (or the same) linear functions, then the unique partitioning provided by ensuing neurons may become less effective, leading to many inputs lying in nearby or the same activation regions even with deeper layers. With positional encoding, the density is alleviated since the distance $\lambda = \|\gamma(x_i) - \gamma(x_j)\|$ for each x_i, x_j is scaled by the frequency, which simultaneously raises its dimensionality and generates more activation regions. The density of inputs can be interpreted through the induced kernel function, which is known to be stationary for positional encoding [23]. This means that the similarity between inputs is only dependent on their distance, inducing a strong diagonal that is missing with coordinate based inputs (Figure 4).

For intuition, we can also relate the density of inputs to the frequency components of the target function. Higher density results in a target function containing higher frequency components, and vice versa. Thus, positional encoding can also be viewed as generating a lower frequency function, which better disperses inputs across available activation regions. This is not possible with the fine-grained sampling of coordinates, as shown in Figures 2 and 3.

4 High Gradient Confusion

In [22], the effect of network architecture on speed of convergence was modeled using gradient confusion, a measure determining the correlation of gradients for differing inputs. It was shown that lower confusion during training can speed convergence of SGD, or make training the network easier. Confusion occurs when two objective functions $\mathcal{L}(f_\theta(x_i), y_i)$ and $\mathcal{L}(f_\theta(x_j), y_j)$, $i \neq j$, have gradients such that $\langle \nabla \mathcal{L}(f_\theta(x_i), y_i), \nabla \mathcal{L}(f_\theta(x_j), y_j) \rangle < 0$. This creates a disagreement on the direction the parameters need to move, slowing down convergence. Convergence rates of SGD were given through the confusion bound $\eta \geq 0$, given as

$$\langle \nabla \mathcal{L}(f_\theta(x_i), y_i), \nabla \mathcal{L}(f_\theta(x_j), y_j) \rangle \geq -\eta$$

for all $i \neq j$ and fixed θ . We focus on this metric since we are interested in the speed at which gradient descent converges and its

relation to the spatial information of the signal.

4.1 Intuition for Higher Confusion

In this section, we aim to build intuition as to why limited expressive power will induce higher amounts of confusion when the target values oscillate rapidly. Assume we are regressing a 1D signal, and let $f^{\mathcal{A}}$ be a linear function given by a ReLU network corresponding to an activation pattern \mathcal{A} . Assume two dense inputs $x_i, x_j \in [0, 1]$ belong to the same $\mathcal{R}(f, \mathcal{A})$. We can then write $x_j = c_0 x_i$, and $\text{sgn}(w_i^{(l)T} (c_i^{l-1} \odot x_i^{l-1}) + b_i^l) = \text{sgn}(w_i^{(l)T} x_i^{l-1} + b_i^l)$ must hold for all neurons, where c^l is a vector of positive values. Therefore,

$$\begin{aligned} \langle \nabla_\theta f^{\mathcal{A}}(x_i), \nabla_\theta f^{\mathcal{A}}(x_j) \rangle &= \\ \langle \nabla_\theta f^{\mathcal{A}}(x_i), d \odot \nabla_\theta f^{\mathcal{A}}(x_i) \rangle &> 0, \end{aligned} \quad (2)$$

where $d \in \mathbb{R}^{\#\text{weights}}$ are the positive values that scale the hidden outputs.

We will now evaluate using Mean Squared Error (MSE) loss

$$\frac{1}{N} \sum_{i=1}^N (y_i - f(x_i))^2.$$

We have the gradient of MSE with respect to the parameters for a single input x as

$$\nabla_\theta \mathcal{L}(f^{\mathcal{A}}(x), y) = -2(y - f^{\mathcal{A}}(x)) \nabla_\theta f^{\mathcal{A}}(x).$$

From (2), we can see that confusion will be directly induced by residual $y - f^{\mathcal{A}}(x)$. If y_i is highly oscillatory for each $x_i \in \mathcal{R}(f, \mathcal{A})$, then confusion will occur in any situation where $y_i > f^{\mathcal{A}}(x_i)$ and $y_j < f^{\mathcal{A}}(x_j)$. Since the direction of the gradient update for each weight is essentially determined by the residual, confusion can only be reduced if the target values change linearly or possibly if constant.

Now, assume we have inputs $x_i, x_j \in [0, 1]$ such that they are regressed by two separate linear functions $f^{\mathcal{A}}$ and $f^{\mathcal{B}}$ of patterns \mathcal{A} and \mathcal{B} . Let $S = \{w_i^l \mid \mathcal{A}_i^l, \mathcal{B}_i^l = 1\}$ denote the set of commonly activated weights between layers. The inner product of the gradients will only depend on the parameters in S since all other weights will cancel out due to ReLU

$$\langle \nabla_S \mathcal{L}(f^{\mathcal{A}}(x_i), y_i), \nabla_S \mathcal{L}(f^{\mathcal{B}}(x_j), y_j) \rangle.$$

While the residual of $\nabla_S \mathcal{L}$ may still be highly oscillatory, it is not necessarily the case that $\langle \nabla_S f^{\mathcal{A}}(x_i), \nabla_S f^{\mathcal{B}}(x_j) \rangle > 0$, as backpropagation will utilize weights $w_i^l \notin S$, the number of which is influenced by the Hamming distance between activation patterns. We can view this as the network utilizing information from distinct activation regions when optimizing shared weights. Essentially, the network can configure the activation regions such that updating shared weights in the same direction can be beneficial for minimizing the loss. The more these patterns are allowed to differ between inputs, the more flexible the network can be when attempting to reduce confusion, while restricting the task to a single activation region provides no flexibility.

4.2 Spectral Bias

The relationship between expressive capacity and confusion is demonstrated by analyzing the confusion densities and Hamming distances

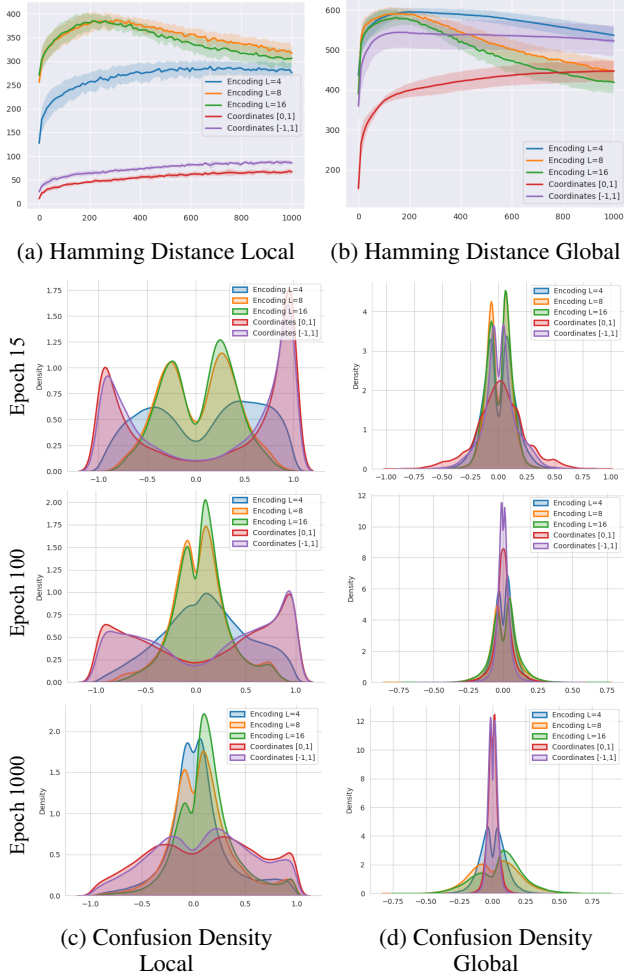


Figure 5: Confusion of gradient descent and hamming distances of activation patterns averaged over 5 natural images. We use inputs sampled in local 50x50 neighborhoods of the image and globally across the image. (a) and (b) plot the hamming distances, while (c) and (d) plot the overall confusion densities. We used 100 local regions, and 50,000 distant pairs. Confusion is measured through the cosine similarity between input gradients pairs.

in Figures 5 and 6. The Hamming distance is a measure of the expressive power between inputs, as it quantifies the dissimilarity of their activation patterns. We compute both confusion and Hamming distance for inputs sampled locally and globally across the signal (i.e., for high and low frequency components, respectively). The pair-wise gradient correlations between inputs at different stages of training are then calculated using cosine similarity, and their densities are plotted. A wider density or higher concentrations in the negative range indicate more confusion, while a density more centered around zero or positive values suggests less confusion. This corresponds to orthogonal or positively correlated gradient directions between inputs.

In Figure 5, we display three key aspects of our observations.

1. Both positional encoding and coordinates are less effective in representing high-frequency components than low-frequency components, as measured by the lower Hamming distances between activation patterns for locally sampled inputs (Fig. 5(a)) in comparison to globally sampled inputs (Fig. 5(b)). As a result, during training, the model gets confused more often when dealing with

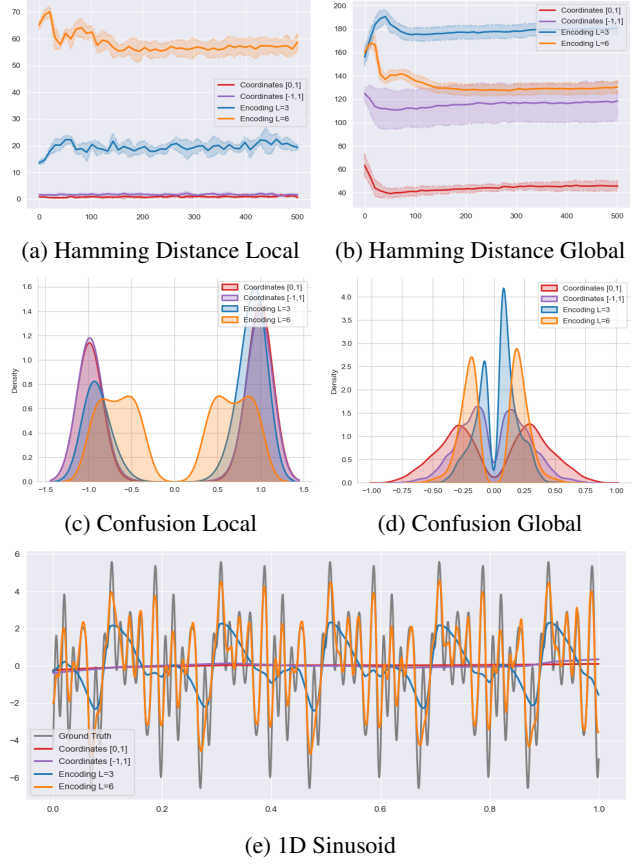


Figure 6: Confusion (epoch 500) and hamming distance conducted on 1D sinusoidal signals. The network is a 4 layer MLP with 128 hidden neurons, results are averaged over five signals. We used 25 local regions of 50 inputs, and 5000 distant pairs.

high-frequency components than low-frequency components (Fig. 5(c)-(d)).

2. Positional encoding endures the least amount of confusion for the high frequency components due to its enhanced expressive capabilities (Fig. 5(a)), which suggests faster convergence.
3. Coordinates generate a large disparity in the quantity of confusion between input samples, which does not occur with positional encoding.

For the 1D sinusoids shown in Figure 6, the same trends hold, but the Hamming distances vary less during training.

Overall, the results demonstrate how each input will likely have its convergence obstructed by its nearest neighbors, caused by the similarity in their activation patterns which induces higher concentrations of confusion. In contrast, distant inputs sampled globally across the signal suffer less confusion since more expressive power can be utilized, resulting in harmonious gradient updates. As a consequence, the network converges faster to the overall structure of the target function than to the local details, resulting in the observed low-frequency representations. Positional encoding allows the network to utilize its enhanced expressive power in an effective manner, granting quicker convergence to the high-frequency components. Moreover, the significant disparity in confusion when using coordinates (between varying frequency components) can be attributed to a larger spectral bias.

While our reasoning should always apply in the uniform case, aspects of these dynamics may differ for inputs of non-uniform distri-

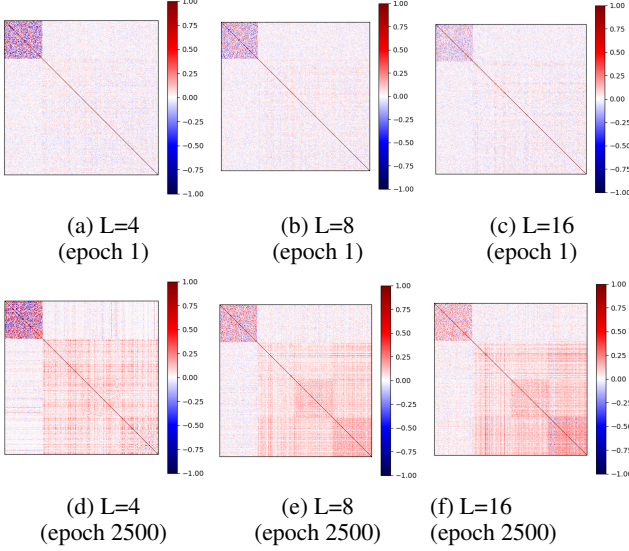


Figure 7: Cosine similarity between hyperplane normals during training across layers. The normal to each hyperplane is simply given as the corresponding weights (Conducted on a single image, holds for other images).

butions, where local densities and their effect on the activation regions will come into play. We also note that more expressive power may not necessarily be more useful if the signal is dominated by low frequency components, where confusion can be avoided easily.

5 Encoding Frequency and Activation Region Properties

We now explore the distinct activation region dynamics induced by higher frequency encodings. Doing so can give more insight into the distinct solutions the network discovers, and may provide preliminary insights on their generalization properties similar to previous works unrelated to spectral bias [7, 26, 16]. We start by analyzing the correlation between hyperplane directions, given as $\nabla_x z(x)$, by taking the cosine similarity between all weights (Figure 7). We find that higher frequency encodings allow for an increase in orthogonal hyperplane directions in the beginning of training (higher dimensional), then become increasingly parallel as training progresses. Specifically, Figure 7 demonstrates that hyperplanes are less negatively correlated in the first layer as the encoding frequency increases, which affects the following layers accordingly.

We find that this behavior results in wider (or larger volume) activation regions later in training, which may counter-intuitively reduce the distinctiveness between activation patterns across the dataset. This reduction in distinctiveness is shown in Figure 5 for higher frequency encodings ($L=8$ and $L=16$), as there is a large dip in the mean Hamming distance. Notice that the low frequency encoding ($L=4$) begins to contract the Hamming distances as well, but at a much slower rate. This may be attributed to the negatively correlated hyperplanes in the first layer, which may restrict the network from quickly finding efficient solutions. To qualitatively demonstrate that the above behavior results in wider activation regions, we visualize 2D slices of the activation regions for a trained network in Figure 8, where the distinction is shown.

Lastly, in Figure 9 we plot the distance of each input to the nearest boundary, given as

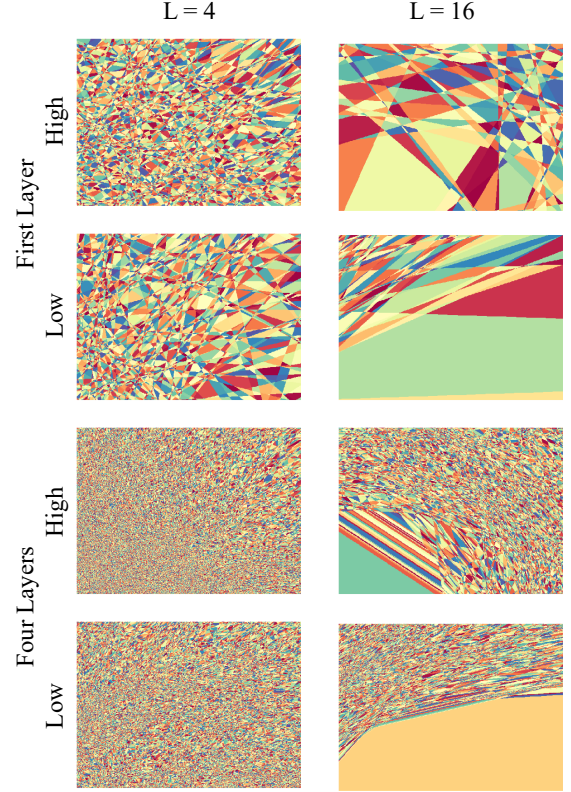


Figure 8: 2D slice of activation regions for high and low frequency encoding after 2500 epochs. Images were found by moving along a 2D plane (all other dimensions fixed) at the origin, with "Low" denoting a 2D plane along the dimensions of the low frequency features of the encoding, and "High" the high frequency features. Visualization done on single image.

$$d(x, \mathcal{B}_f) = \min_{z(x) \in f} |z(x) - b_z| / \|\nabla z(x)\|,$$

originally shown in [7]. This distance measures the sensitivity of neurons to the given input samples, or in other words sensitivity to boundary transitions. Note that wider regions may lead to an increase of this distance, but should not directly induce it. In Figure 9, the higher frequency encodings first have a larger contraction of this distance, then rapidly increase it during training, indicating a shift from high to low sensitivity. This measure is interesting as it was used in [7] for the MNIST dataset, where a similar behavior was found. They discovered that the network will quickly contract the distances, which is correlated with better generalization performance towards the end of training. However, we also notice an increase after this contraction which is larger for higher frequency encodings. Different sensitivity measures have previously been used in discussions regarding generalization (and linear regions) as well, similar to the above metric [16, 15]. Although, the relationship between each measure is still unclear.

Overall, networks using higher frequency encodings tend to find solutions in which many hyperplanes are highly correlated, which simultaneously increases the volume of the activation regions and reduces the sensitivity of neurons to the input samples later in training. These properties can be linked to faster convergence to the target signal as shown in Section 4, and is not obtained by lower frequency encodings. However, these solutions may hinder generalization per-

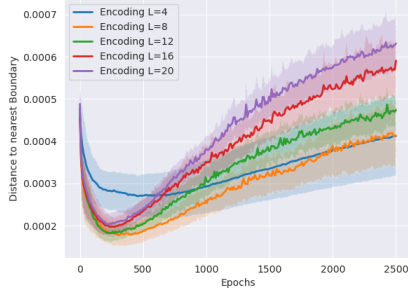


Figure 9: The mean distance of training points to boundaries \mathcal{B}_f of ReLU neurons. This gives a measure of the sensitivity of neurons to the inputs samples during training, and how this fluctuates.

formance, since higher frequency encodings are known to overfit [23]. We believe the connection between these properties and the generalization of positional encoding can be further explored.

6 Dying ReLU

Although coordinate based networks slowly increase the number of activation regions throughout training as shown in Figure 3 (b), there is a surprising alternative that is simultaneously occurring. That is, the network is increasingly *shutting off* ReLU neurons during training, limiting its full expressive potential while simultaneously attempting to utilize different linear functions with available neurons. We believe this is due to the exponential increase in parameter norms that occur when training on high frequency target functions, which can cause issues due to the density of the data.

We computed the parameter norms $\prod_{n=1}^L \|\mathbf{W}^{(k)}\|$ across layers, where $\|\cdot\|$ is the spectral norm found by the maximum singular value, displayed in Figure 10. This norm represents the upper bound of the Lipschitz constant L_f of the network, and it may be slightly counter-intuitive to see that this bound is higher for the network with a larger spectral bias. It is also interesting to see the difference in layer norms with choice of input (Fig. 10(a)-(b)).

In this setting, it may be the case that larger parameters can easily map coordinates to one side of the bias threshold, causing it to be inactive for the rest of training. We can see some intuition for this idea from Figure 10 (d). The number of dead ReLU neurons decreases as the normalizing interval increases, meaning once the data becomes less dense there are more active neurons. While this may be the case, there is still the overall trend of an increasing amount of dead neurons, which displays another limitation of ReLU networks in this dense, low dimensional setting. Additionally, this seems to be an issue at initialization, which can perhaps be reduced with proper weight initialization, or other potential measures.

7 Conclusion and Future Work

In this paper, we provided a thorough study of spectral bias in the coordinate based setting by using a direct model of training dynamics. This analysis provides the first look into the properties of the network that induce spectral bias without the use of NTK or Fourier analysis. We found that convergence of gradient descent in local regions of input space, which utilize less expressive capacity for neighboring inputs, is slower in comparison to inputs sampled globally across the signal. This results in the high frequency details of the signal being learned after a low frequency representation is achieved, with the severity of spectral bias depending on how the network assigns

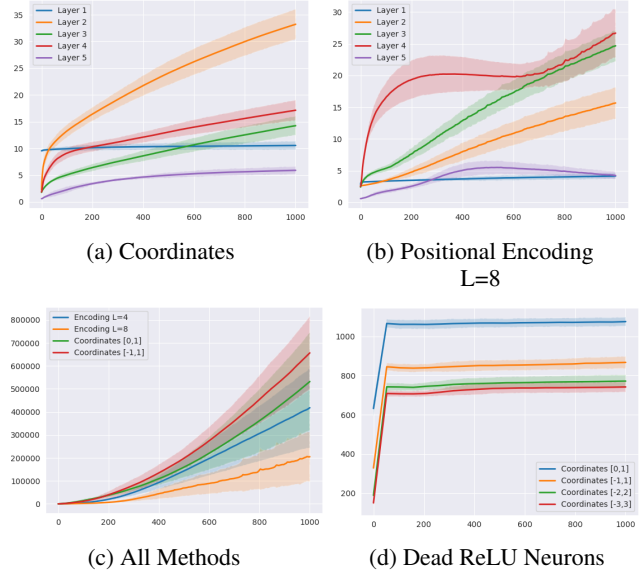


Figure 10: Spectral norm for both positional encoding ($L=8$) (b) and coordinates ($[0,1]$) (a) throughout training (a-c), along with the amount of dead ReLU neurons during training for coordinates (d). There are no dead ReLU neurons for positional encoding.

inputs to activation regions. Positional encoding is able to enhance expressive capacity overall, which can result in faster convergence to the high frequency components. In addition to this, we explored the properties of the activation regions as encoding frequency increases, which gains insight into the differing solutions the network arrives at. Lastly, another limitation of ReLU in this low dimensional setting comes from the dying ReLUs, which are most likely caused by the density of inputs and the exponential increase in parameter norms.

Our analysis not only provides a new interpretation of spectral bias, but also exposes its severity in dense settings. We hope that the relationship between expressive capacity and gradient descent convergence can be extended to explore spectral bias in non-uniform settings with different objectives such as classification. We also hope that this approach can help provide more insight as to how spectral bias impacts generalization in ReLU networks, in which analyzing the properties of the activation regions may provide a unique approach.

References

- [1] Eiríkur Agustsson and Radu Timofte, ‘Ntire 2017 challenge on single image super-resolution: Dataset and study’, in *The IEEE Conference on Computer Vision and Pattern Recognition (CVPR) Workshops*, (July 2017).
- [2] David Balduzzi, Marcus Frean, Lennox Leary, JP Lewis, Kurt Wan-Duo Ma, and Brian McWilliams, ‘The shattered gradients problem: If resnets are the answer, then what is the question?’, (2017).
- [3] Ronen Basri, Meirav Galun, Amnon Geifman, David Jacobs, Yoni Kasten, and Shira Kritchman, ‘Frequency bias in neural networks for input of non-uniform density’, in *International Conference on Machine Learning*, pp. 685–694. PMLR, (2020).
- [4] Yuan Cao, Zhiying Fang, Yue Wu, Ding-Xuan Zhou, and Quanquan Gu, ‘Towards understanding the spectral bias of deep learning’, in *Proceedings of the Thirtieth International Joint Conference on Artificial Intelligence, IJCAI-21*, ed., Zhi-Hua Zhou, pp. 2205–2211. International Joint Conferences on Artificial Intelligence Organization, (8 2021). Main Track.
- [5] Rizal Fathony, Anit Kumar Sahu, Devin Willmott, and J Zico Kolter, ‘Multiplicative filter networks’, in *International Conference on Learning Representations*, (2021).

- [6] Stanislav Fort, Paweł Krzysztof Nowak, Stanisław Jastrzebski, and Srinu Narayanan. Stiffness: A new perspective on generalization in neural networks, 2019.
- [7] Boris Hanin and David Rolnick, ‘Complexity of linear regions in deep networks’, in *Proceedings of the 36th International Conference on Machine Learning*, eds., Kamalika Chaudhuri and Ruslan Salakhutdinov, volume 97 of *Proceedings of Machine Learning Research*, pp. 2596–2604. PMLR, (09–15 Jun 2019).
- [8] Boris Hanin and David Rolnick, *Deep ReLU Networks Have Surprisingly Few Activation Patterns*, Curran Associates Inc., Red Hook, NY, USA, 2019.
- [9] Arthur Jacot, Franck Gabriel, and Clément Hongler, ‘Neural tangent kernel: Convergence and generalization in neural networks’, *Advances in neural information processing systems*, **31**, (2018).
- [10] Jonas Kiessling and Filip Thor, ‘A computable definition of the spectral bias’, **36**, 7168–7175, (Jun. 2022).
- [11] Diederik P. Kingma and Jimmy Ba, ‘Adam: A method for stochastic optimization’, in *3rd International Conference on Learning Representations, ICLR 2015, San Diego, CA, USA, May 7-9, 2015, Conference Track Proceedings*, eds., Yoshua Bengio and Yann LeCun, (2015).
- [12] Lars Mescheder, Michael Oechsle, Michael Niemeyer, Sebastian Nowozin, and Andreas Geiger. Occupancy networks: Learning 3d reconstruction in function space, 2018.
- [13] Ben Mildenhall, Pratul P. Srinivasan, Matthew Tancik, Jonathan T. Barron, Ravi Ramamoorthi, and Ren Ng. Nerf: Representing scenes as neural radiance fields for view synthesis, 2020.
- [14] Guido F Montufar, Razvan Pascanu, Kyunghyun Cho, and Yoshua Bengio, ‘On the number of linear regions of deep neural networks’, in *Advances in Neural Information Processing Systems*, eds., Z. Ghahramani, M. Welling, C. Cortes, N. Lawrence, and K.Q. Weinberger, volume 27. Curran Associates, Inc., (2014).
- [15] Behnam Neyshabur, Srinadh Bhojanapalli, David McAllester, and Nati Srebro, ‘Exploring generalization in deep learning’, in *Advances in Neural Information Processing Systems*, eds., I. Guyon, U. Von Luxburg, S. Bengio, H. Wallach, R. Fergus, S. Vishwanathan, and R. Garnett, volume 30. Curran Associates, Inc., (2017).
- [16] Roman Novak, Yasaman Bahri, Daniel A. Abolafia, Jeffrey Pennington, and Jascha Narain Sohl-Dickstein, ‘Sensitivity and generalization in neural networks: an empirical study’, *ArXiv*, **abs/1802.08760**, (2018).
- [17] Razvan Pascanu, Guido Montufar, and Yoshua Bengio. On the number of response regions of deep feed forward networks with piece-wise linear activations, 2013.
- [18] Maithra Raghu, Ben Poole, Jon Kleinberg, Surya Ganguli, and Jascha Sohl-Dickstein, ‘On the expressive power of deep neural networks’, in *Proceedings of the 34th International Conference on Machine Learning - Volume 70, ICML’17*, p. 2847–2854. JMLR.org, (2017).
- [19] Nasim Rahaman, Aristide Baratin, Devansh Arpit, Felix Draxler, Min Lin, Fred Hamprecht, Yoshua Bengio, and Aaron Courville, ‘On the spectral bias of neural networks’, in *International Conference on Machine Learning*, pp. 5301–5310. PMLR, (2019).
- [20] Ali Rahimi and Benjamin Recht, ‘Random features for large-scale kernel machines’, in *Advances in Neural Information Processing Systems*, eds., J. Platt, D. Koller, Y. Singer, and S. Roweis, volume 20. Curran Associates, Inc., (2007).
- [21] Basri Ronen, David Jacobs, Yoni Kasten, and Shira Kritchman, ‘The convergence rate of neural networks for learned functions of different frequencies’, in *Advances in Neural Information Processing Systems*, eds., H. Wallach, H. Larochelle, A. Beygelzimer, F. d’Alché-Buc, E. Fox, and R. Garnett, volume 32. Curran Associates, Inc., (2019).
- [22] Karthik A. Sankararaman, Soham De, Zheng Xu, W. Ronny Huang, and Tom Goldstein, ‘The impact of neural network overparameterization on gradient confusion and stochastic gradient descent’, in *Proceedings of the 37th International Conference on Machine Learning, ICML’20*. JMLR.org, (2020).
- [23] Matthew Tancik, Pratul Srinivasan, Ben Mildenhall, Sara Fridovich-Keil, Nithin Raghavan, Utkarsh Singhal, Ravi Ramamoorthi, Jonathan Barron, and Ren Ng, ‘Fourier features let networks learn high frequency functions in low dimensional domains’, *Advances in Neural Information Processing Systems*, **33**, 7537–7547, (2020).
- [24] Zhi-Qin John Xu, ‘Frequency principle: Fourier analysis sheds light on deep neural networks’, *Communications in Computational Physics*, **28**(5), 1746–1767, (jun 2020).
- [25] Dong Yin, Ashwin Pananjady, Max Lam, Dimitris Papailiopoulos, Kannan Ramchandran, and Peter Bartlett, ‘Gradient diversity: a key ingredient for scalable distributed learning’, in *Proceedings of the Twenty-First International Conference on Artificial Intelligence and Statistics*, eds., Amos Storkey and Fernando Perez-Cruz, volume 84 of *Proceedings of Machine Learning Research*, pp. 1998–2007. PMLR, (09–11 Apr 2018).
- [26] Xiao Zhang and Dongrui Wu, ‘Empirical studies on the properties of linear regions in deep neural networks’, *ArXiv*, **abs/2001.01072**, (2020).